Title

Biocompatibility of a Synthetic Biopolymer for the Treatment of Rhegmatogenous Retinal Detachment

Journal

Journal of Clinical & Experimental Ophthalmology, 2015(5)

ISSN

2155-9570

Authors

Sarfare, Shanta
Dacquay, Yann
Askari, Syed
et al.

Publication Date

2015-10-01

DOI

10.4172/2155-9570.1000475

Peer reviewed

Published in final edited form as:

J Clin Exp Ophthalmol. 2015 October ; 6(5): . doi:10.4172/2155-9570.1000475.

Biocompatibility of a Synthetic Biopolymer for the Treatment of Rhegmatogenous Retinal Detachment

Shanta Sarfare[1,*], **Yann Dacquay**[1], **Syed Askari**[2], **Steven Nusinowitz**[1], and **Jean-Pierre Hubschman**[1]

[1]Jules Stein Eye Institute, David Geffen School of Medicine, University of California at Los Angeles, Los Angeles, California 90095, USA

[2]Medicus Biosciences, 2528 Qume Drive, Unit 1, San José, California 95131, USA

Abstract

Objective—The aim of this study is to evaluate the retinal safety and toxicity of a novel synthetic biopolymer to be used as a patch to treat rhegmatogenous retinal detachment.

Methods—Thirty one adult wild type albino mice were divided in 2 groups. In Group A (n=9) 0.2 µl balanced salt solution (BSS) and in Group B (n=22), 0.2 µl biopolymer was injected in the subretinal space. Trans-scleral subretinal injection was performed in one eye and the fellow eye was used as control. In both groups, in vivo color fundus photography, electroretinogram (ERG), spectral domain optical coherence tomography (SD-OCT) were performed before injection and at days 7 and 14 post-intervention. Histological analysis was performed following euthanization at days 1, 7 and 21 post-injection.

Results—The biopolymer was visualized in the subretinal space in vivo by SD-OCT and post-life by histology up to 1 week after the injection. There were no significant differences in ERG parameters between the two groups at 1 and 2 weeks post-injection. Minimal inflammatory response and loss of photoreceptor cells was only observed in the immediate proximity of the site of scleral perforation, which was similar in both groups. Overall integrity of the outer, inner retina and retinal pigment epithelial (RPE) layers was unaffected by the presence of the biopolymer in the subretinal space.

Conclusions—Functional and histological evaluation suggests that the synthetic biopolymer is non-inflammatory and non-toxic to the eye. It may represent a safe therapeutic agent in the future, for the treatment of rhegmatogenous retinal detachment.

[*]**Corresponding author:** Shanta Sarfare, Ora, Inc., 300 Brickstone Square, Andover, Massachusetts, USA, Tel: 978-685-8900 extension 9532; Fax: 978-689-0020; ssarfare@gmail.com.

Citation: Sarfare S, Dacquay Y, Askari S, Nusinowitz S, Hubschman JP (2015) Biocompatibility of a Synthetic Biopolymer for the Treatment of Rhegmatogenous Retinal Detachment. J Clin Exp Ophthalmol 6: 475. doi: 10.4172/2155-9570.1000475

Financial Disclosure

Syed Askari is the founder and employee of Medicus Biosciences. All other authors have no conflict of interest or financial disclosures.

Keywords

Retinal detachment; Retinal adhesive; Retinal tear

Introduction

Retinal detachment is the separation of the neurosensory retina from the RPE, and is a potentially blinding ocular condition. Rhegmatogenous retinal detachments are the most common type of retinal detachments and are secondary to retinal holes and/or breaks, which allow fluid from the vitreous cavity to enter the space between the RPE and the neurosensory retina. Individuals with myopia, as well as history of cataract surgery, trauma or ocular infections have a higher risk of developing rhegmatogenous retinal detachment [1-3]. Left untreated, a chronic retinal detachment can lead to complications such as proliferative vitreoretinopathy (PVR), vision loss and permanent blindness [4].

Standard treatment for rhegmatogenous retinal detachment involves scleral buckling and/or pars plana vitrectomy (PPV). Endotamponade agents such as air, sulfur hexafluoride (SF6), octafluoropropane (C3F8) gas or silicone oil are used to maintain the retina in place and reduce fluid flow through the retinal opening until the retinopexy scar heals [5-8]. Although tamponade agents are successful in achieving reattachment, they have several disadvantages such as head positioning, travel restrictions, limited vision for up to 2 months, silicone oil adhesion to intraocular lenses, cataract, glaucoma, keratopathy and need for second surgery [9-13].

Some retinal adhesive products have been previously tested [14-20]. The advantage of using retinal adhesives is that they can be used as a patch to cover and seal the retinal holes and/or retinal breaks and eliminate the need for gas or silicone oil tamponade. However, these agents demonstrated severe retinotoxicity, inflammatory reaction, difficulty of delivery or limited efficacy [14,15,17,19]. There is currently no product available that is non-toxic to the ocular structures and which has the ability to effectively seal the retinal breaks in retinal detachment surgery.

Polyethylene glycol (PEG) derivatives with molecular weights 10 kilo Dalton (kDa) and higher are generally recognized as safe and nontoxic [20] and therefore have been extensively used in medical devices and as drug carriers in pharmaceuticals applications [21-23]. Our study aims to evaluate the potential ocular and in particular the retinal toxicity of a PEG-derived ophthalmic biopolymer through clinical, electrophysiological and histological evaluations.

Methods

Animals

Albino Balb/c mice 6–8 weeks of age purchased from Jackson Laboratories, ME maintained on 12/12 hours light/dark cycle were used in this study. All experiments were performed with IACUC-approved protocols and following the ARVO Statement for the Use of Animals in Ophthalmic and Vision Research.

Generation of the ophthalmic biopolymer

The ophthalmic pre-formulation developed by Medicus Biosciences (San José, California) comprises of three compounds: one containing 8 nucleophilic groups (8-arm-PEG 20K amine), the second also containing 8 nucleophilic groups and 8 degradable acetate groups (8-arm-PEG 20K amine acetate) and the third containing 4 electrophilic groups (4-arm-PEG 20K amide ester) in a stoichiometric ratio; an aqueous buffer and a viscosity enhancer [24-27]. The polymer was designed to be degraded in 2-weeks by selecting degradable acetate groups, numbers of crosslinking sites and the polymer concentration in the solution. Retinal adherence and the viscosity of the polymer were enhanced with the use of hydroxyl methyl propyl methyl cellulose. The polymer demonstrated in previous study similar adhesive properties as the retina when tested in our laboratory [28]. All reactive PEG materials were purchased from JenKem Corp, Plano, Texas. The firmness, adhesion, and elastic modulus of the polymer were characterized by a Texture Analyzer (TA.XT.plus) with Exponent software (v6.0) using various probes. The components in the injection kit were mixed, filtered and injected into the subretinal space as a liquid biopolymer which solidifies at pH 7.4 at a pre-set time of 90–300 sec and adheres to the tissue.

Subretinal injections

Eyes were dilated with 2.5% phenylephrine (HUB Pharmaceuticals, Rancho Cucamonga, CA) and 0.5% tropicamide (Akorn Pharmaceuticals, Lake Forest, IL). Mice were anesthetized with ketamine (100 mg/kg; Phoenix Pharmaceuticals) and xylazine (8 mg/kg; Lloyd Laboratories). Goniovisc (2.5%) (HUB Pharmaceuticals, Rancho Cucamonga, CA) was applied to the eye to maintain corneal clarity and optical interface. Of the 31 mice in the study, 9 mice were assigned to Group A (subretinal BSS) and 22 mice to Group B (subretinal biopolymer). 0.2 μl biopolymer or BSS was injected in one eye for each mouse of the two groups and the non-injected fellow eye was used as control.

Fluorescein to a final concentration of 0.01% was co-injected to facilitate visualization during injection. A multi-purpose rigid telescoping endoscope (11 cm length × 2.7 mm diameter) with a 30° beveled tip (Karl Storz, Tuttlingen, Germany) was used for direct visualization while performing the subretinal injections. The endoscope tip was illuminated via a fiber optic cable connected to a xenon light source (Xenon Nova 175, Karl Storz, Tuttlingen, Germany) and connected to a high definition camera and monitor (IMAGE 1 HUB, Karl Storz, Tuttlingen, Germany). The endoscope tip was apposed to the corneal surface, while the injection was performed with a trans-scleral/choroidal approach using a 33 g beveled needle attached to a 10 μl Nanofil syringe (World Precision Instruments, Sarasota, FL).

Imaging

Fundus imaging—Mice were anesthetized with 5% isoflurane (Abbott Laboratories, Abbott Park, IL) and visualization was performed with the endoscope camera as described above.

Spectral domain optical coherence tomography (SD-OCT)—Ultra high resolution SD-OCT imaging was performed on both eyes from all groups, at baseline 1 week prior and

1 and 2-weeks post-injection using Bioptigen SD-OCT system (Research Triangle Park, NC). A series of 100 b-scans were collected, stacked and aligned spatially to form a registered three-dimensional rendering of retinal volume.

Functional evaluation

Electroretinography (ERG)—Dark adapted rod-mediated ERGs were recorded to blue flashes (Wratten 47A, λ_{max}=470 nm). Bilateral ERG recordings were performed on 16 mice, at baseline 1 week prior and 1 and 2-weeks post injection, as previously described [29]. ERGs were recorded from the cornea using a gold loop electrode, referenced to a similar gold wire in the mouth. The mouse eye was positioned in front of an opening in a large integrating sphere in which brief flashes of light at 1 Hz interval were presented. Responses were amplified 10,000 × (Grass P511 High Performance AC Amplifier), band-pass filtered (0.1-300 Hz), digitized using an I/O board (PCI-6221; National Instruments, Austin, TX) and averaged.

Histological evaluation—Light, electron microscopy and immunocytochemistry.

Paraffin embedded tissue (FFPE)—Eyes from mice (group A, n=3; group B, n=13) 3 weeks post-injection were fixed in 10% neutral buffered formalin, paraffin embedded and sectioned. Consecutive 5-μm sections were stained with hematoxylin and eosin (H&E) for light microscopy and processed for TUNEL labeling or immunohistochemistry.

Plastic embedded tissue—Mouse eyes (group A, n=3; group B, n=6) were oriented with respect to site of injection using cautery iron or tissue marker pen, fixed with a mixture of 2% paraformaldehyde: 2.5% glutaraldehyde in 0.1M sodium phosphate buffer (pH 7.4) and processed as previously described [30]. Sections of 1μm thickness stained with Toluidine blue were imaged with a Zeiss Axiophot microscope and ultra-thin sections stained with uranium and lead salts were imaged using Zeiss EM910 electron microscope.

Terminal deoxynucleotidyl transferase (TdT)-mediated dUTP nick-end-labeling (TUNEL)

At 3 weeks post-injection, DNA fragmentation was detected using the DeadEnd Colorimetric TUNEL System (Promega, Madison, WI) and light microscopy according to the manufacturer's protocol. Two sections from 3 eyes in each group were labeled and nuclei were counterstained with 4′,6-diamidino-2-phenylindole (DAPI).

Immunohistochemistry

Two eyes from each group were oriented with cautery iron and/or tissue marker pen, fixed in 4% paraformaldehyde, cryopreserved and sectioned using standard protocols as previously described [31]. Sections were stained with anti-rhodopsin (ab3267, Abcam); anti-GFAP (ab53554, Abcam); anti-Iba1 (019-19741, Waco); anti-F4/80 (MCA497GA, AbD Serotec) primary antibodies and Alexa 488-labeled anti-mouse; anti-rat and anti-rabbit secondary antibodies (Molecular Probes, Life technologies), counterstained with DAPI (Molecular Probes, Life technologies) and imaged using Olympus Fluoview FV1000 Laser Scanning Confocal microscope.

Results

Color fundus imaging of subretinal bleb

Due to co-injection of fluorescein with the biopolymer, a hyper fluorescent spot with a distinct outline marking the detachment can be seen in subretinal biopolymer injected eyes (Figure 1). The retinal vessels are clearly seen in front of the hyper fluorescent area, indicating a true subretinal injection without leakage in the vitreous space. In fellow eyes with no injections, there is no sign of retinal change. The fluorescein cleared rapidly and the subretinal blebs start regressing in 24-48 hours post-injection. Fundus imaging at 1 week post-injection showed a bright reflective area with raised edges or ruffles matching the size of the detachment produced by the biopolymer injection.

SD-OCT imaging of retinal structure

Bilateral SD-OCT imaging encompassing the detached and neighboring attached retina was performed for all mice 1 and 2 weeks post-injection. Local disruption of the retinal layers was seen at the site of the needle puncture wound for all injected eyes (Figure 2). In biopolymer injected eyes, a small detachment persisted 1 week post-injection (Figure 2C) whereas in the BSS injected eyes, the retina was completely re-attached (Figure 2B). The photoreceptor and RPE layers were disrupted directly under the detachment and hyporeflective material corresponding to the biopolymer and hyperreflective cellular debris could be seen under the retina. There was no evidence of any abnormalities in the lens, vitreous and anterior segment structures in any of the injected groups.

Histology of mouse eyes following subretinal injection

Light microscopy—We examined perfusion-fixed, plastic embedded and Toluidine-blue stained sections of both injected and non-injected eyes at 1 day post-injection. Compared to the non-injected eyes (Figures 3A and 3D), the BSS-injected eyes showed some disorganization of the photoreceptor outer segments and vacuoles in the RPE layer (Figures 3B and 3E). In the subretinal biopolymer injected eyes, the biopolymer could be seen as Toluidine blue-stained amorphous material in the subretinal space 1 day post-injection (Figures 3C and 3F). At this time point, the photoreceptor outer segments overlying the detachment appeared compressed and partially disorganized but the inner segments and rest of the retinal morphology appeared normal in both BSS and biopolymer injected eyes. Occasional rounded macrophage-like cells could be seen infiltrating into the biopolymer layers from the RPE-choroidal layer at this stage (Figure 3G). Retinal morphology was completely normal immediately adjacent to the detachment in the subretinal biopolymer injected eyes (Figure 3H).

We examined eyes from H&E stained FFPE sections from all injected groups 3 weeks post-injection. The retina of the BSS injected eyes appeared normal (Figures 4A and 4C). As expected, the biopolymer could not be detected in the subretinal or vitreous space at this time point (Figures 4B and 4D). A sharp demarcation was seen between the site of needle entry causing physical damage to the overlying retina and the adjoining retina which appeared normal. At the needle entry site in the retina, H&E staining revealed destruction of the outer retina and rounded RPE or macrophage-like cells in the subretinal space, consistent

with surgical damage to the retina from needle entry and liquid pressure from the injection, whereas no such changes were seen outside the injection site. The anterior segment and lens appeared normal in all groups.

Electron microscopy—In order to examine in greater detail the effect of biopolymer on RPE and its recovery after reattachment, we used transmission electron microscopy to observe the ultrastructure of the RPE and subretinal space. The retina appears reattached 1 day post-injection of BSS (Figure 5B). In control non-injected (Figure 5A) and subretinal BSS-injected eyes (Figure 5B), the rod outer segments are close to the RPE monolayer with the tips of the outer segments enclosed by the apical processes of the RPE. 1 day after injection of biopolymer in the subretinal space, amorphous “blobs” (p) of biopolymer are seen overlying the RPE (Figure 5C). The RPE apical microvilli (v) appear shorter and compressed consistent with temporary remodeling due to retinal detachment [32]. When assessed at 3 weeks post-injection of biopolymer, the RPE apical microvilli once again appear normal, the biopolymer has been absorbed and the photoreceptor outer segments (os) are apposed to the RPE (Figure 5D).

Apoptotic or necrotic cell death determination by TUNEL staining

We assessed ongoing apoptotic cell death at three weeks post-injection by TUNEL staining. Extremely sparse TUNEL-positive nuclei were observed exclusively in the outer nuclear layer (ONL) of both non-injected and BSS-injected eyes (Figure 6). In the biopolymer injected eyes, apoptotic nuclei were observed in the photoreceptor layer only at the needle puncture site with none to extremely sparse TUNEL labeling in the retina distal to the injection site.

Photoreceptor recovery and inflammatory markers

We examined sections containing the injected quadrant of the eye for markers of photoreceptor recovery and inflammation 1 week post-injection. Proper localization of rhodopsin to the photoreceptor outer segments was observed in the biopolymer injected eyes (Figures 7A and 7B). Equitable distribution of retinal glial cells (microglia; macroglia) which produce inflammatory cytokine as visualized with the marker Ionized calcium binding adaptor molecule1 (Iba1) was observed in both the control BSS-injected and biopolymer-injected eyes (Figures 7C and 7D). No evidence of these phagocytic microglia was observed in the outer or inner nuclear layer. Immunoreactivity for pan-macrophage marker F4/80 is seen in subpopulations of phagocytic microglia in several retinal degenerative diseases [33], ischemia-induced retinopathy [34] and laser-induced retinal injury models [35]. However F4/80-reactive macrophages were not observed in the retina or the subretinal space of either BSS-injected or biopolymer-injected eyes (Figures 7E and 7G). F4/80-positive microglia/macrophages were normally observed in the ciliary body from the same sections (Figures 7F and 7H), as has been previously reported in wild-type mouse retina [36,37].

To determine gliosis, we used the marker for glial fibrillary acidic protein (GFAP) which labels the Müller cell “endfeet” and astrocytes in the inner limiting membrane and nerve fiber layer (NFL). GFAP labeling was observed in the NFL corresponding to the distribution

of retinal astrocytes and Müller cell “endfeet” in control non-injected and BSS-injected eyes (Figures 7I and 7J). In the biopolymer-injected eyes, minimally increased GFAP reactivity was seen at the site of the needle stick (Figure 7K), but GFAP labeling remained normal at all sites immediately distal from the site of needle stick (Figure 7L).

Effect of biopolymer on retinal function

Dark-adapted ERGs were recorded at baseline, and at 1- and 2-weeks post-injection. Rod b-wave amplitudes as a function of retinal illuminance were analyzed by finding the parameters of the best fit using the Naka-Rushton function as previously described [38]. We assessed potential retinal toxicity of the biopolymer by comparing the interocular difference in V_{max}, the maximum saturated b-wave response before and after injections, to the interocular difference in V_{max} at baseline for each mouse. Vmax at baseline, expressed as a percentage difference, ΔV_{max}%, was not statistically significant between eyes (ΔV_{max}=0.67%, t=0.32, df=17, P=0.75).

For group A (subretinal BSS), there was a slight weakening of function in the injected eye at 1-week post injection, although the change in V_{max} was not statistically significant (df=23, ΔV_{max}=−3.3%, t=0.76, P>0.48). (In this and in subsequent analyses, a “-”ΔVmax indicates that the injected eye performed worse than the non-injected control eye.) Although the number of eyes tested at 2-weeks post injection was small (n=3) there is a suggestion of continued weakening of the response (ΔVmax=−8.70%, no statistical test was performed due to the small number of mice tested).

For group B (subretinal polymer), ERGs were performed at baseline and again at 1- and 2-weeks post injection. There was no significant change in retinal function at 1-week (ΔV_{max}= −0.82%, tpaired=1.13, P>0.28) or at 2-weeks post injection (ΔV_{max}=−11.47%, tpaired=0.76, P>0.48). Overall, retinal function for the subretinal polymer injected eyes at 1- and 2- weeks post injection did not change significantly from baseline.

Discussion

Retinal breaks or holes combined with vitreoretinal tractional forces are the causes of rhegmatogenous retinal detachments [39]. The annual incidence of retinal detachment is 1 in 10,000 or 1 in 300 over the lifetime [1,40,41], often requiring therapeutic surgery to prevent permanent loss of vision. These retinal openings allow vitreous fluid to enter the subretinal space and enlarge the retinal detachment. Over time, loss of contact of the photoreceptor layer with the supporting RPE starts a cascade of processes leading to Müller glia proliferation and ultimately photoreceptor cell death and vision loss [42,43]. Additionally, RPE cells can migrate into the vitreous through the break in the retina where they can release inflammatory cytokines and cause proliferation of epiretinal and subretinal membranes described as PVR [44,45]. PVR is a major complication of retinal detachment surgery, exerting traction on the retina and causing recurrent retinal detachment [46,47]. Currently laser photocoagulation is used during PPV surgery to create chorioretinal adhesion around the retinal break, and silicone oil or gas tamponade agents are used to fill the vitreous cavity and keep the neuroretina attached to the RPE until the retinopexy becomes effective [5-8,48-50]. These tamponade agents cause considerable patient discomfort and

complications [51]. Additionally, it takes up to 2 weeks for the laser scar to develop, during which time the unsealed tear may allow the release of RPE, inflammatory cells and serum components from the subretinal space into the vitreous [52,53].

A retinal adhesive is designed to be used during surgery to form a temporary seal of the retinal tear, which eliminates the fluid flow from the vitreous cavity into the subretinal space and also prevent RPE migration into the vitreous while the laser retinopexy takes effect [54]. This would eliminate the need for long-term tamponade agents. A successful retinal patch must stick to the retinal surface, seal the tear and remain in place until the retinopexy is effective. It would also be advantageous it this polymer can be applied to the retinal site through a 23-27 gauge cannula as a liquid and polymerize in vivo. Previously, cyanoacrylate or fibrin-based glues, mussel protein adhesive and other hydrogels have been tested in animal models or clinical cases for the treatment of retinal detachment [14-19]. These agents have limitations such as severe retinotoxicity, inflammation, difficulty of delivery or limited efficacy.

Medicus Biosciences has developed a novel PEG-derived adhesive biopolymer having the mechanical properties required to seal the retinal tears and avoiding the complications of current treatments. The reactants can be in vivo polymerized in PBS at physiological pH. Reacting liquid monomers injected at the site of the retinal break would adhere to the retinal surface and seal the lesion when gelled at a predetermined time. Medicus has manipulated the viscoelastic properties of the biopolymer such that it behaves identically to the healthy human retina [55]. The biopolymer can be delivered as a liquid through conventional minimally invasive instrumentation found in ophthalmological operating rooms, allowing sufficient working time for application to multiple, large retinal breaks. The transparency of the adhesive should allow maintenance of visual function of the patient in case the biopolymer needs to be used in the macular area. The biopolymer dissolves in about 2 weeks after application leaving no permanent residue. The kinetics of the polymerization and disaggregation can be easily modified and controlled to be adapted to the needs. This allows for maintaining the neuro-retina attached to RPE and re-establishment of normal photoreceptor outer segment-RPE connections.

Since the adhesive is designed to be delivered to the retinal surface during vitreo-retinal surgery, we decided to examine the safety and toxicity of the biopolymer when in direct contact with the mouse retina. Although the best way to avoid possible positive or negative effects of melanin on oculotoxicity is to test both pigmented and non-pigmented animals [56], we used albino mice in this study as lack of pigment in the RPE and choroid allowed for easier visualization of the needle tip during the trans-scleral injection approach for delivery in the subretinal space.

To test the retinal toxicity of the polymer, we decided to inject the biopolymer in the subretinal space using a trans-scleral approach. We understand that, in the normal life, this polymer will be delivered mainly on the retinal surface through the vitreous cavity, with only a limited amount accessing the subretinal space through the retinal opening. We decided to consider this approach given the very large relative size of the mouse lens and the fact that the vitreous in mice is firmly attached to the retina. In this model, an intravitreal

injection of the polymer would have been impossible and would not allow direct contact of the polymer with the retinal surface. We observed slightly weaker ERG responses in all injected eyes including BSS controls, which we attribute to traumatic damage to the small mouse eye from the injection itself. There was no significant reduction in ERG parameters due to the biopolymer and our functional assays were not consistent with a toxic response to the biopolymer.

We show that the biopolymer is safe, well-tolerated and causes no inflammatory response or retinal abnormalities. Clumps of dislodged RPE cells and photoreceptor outer segment debris that can be seen under the detachment are attributed to mechanical damage caused by injection pressure [57]. Proliferation of Müller glial cells recognized by GFAP upregulation is observed in retinal inflammation due to various stress stimuli [32,58-60]. In the biopolymer-injected eyes we observed no signs of glial proliferation outside the immediate site of needle entry wound. Loss of photoreceptors was observed in both experimental as well as BSS control eyes in front of the site of sclerochoroidal perforation, indicating that it is from the physical trauma of the injection and not related to the biopolymer itself. Photoreceptor cell death by apoptosis peaks at 3 days after retinal detachment and gradually diminishes [61]. Three weeks after biopolymer injection in the subretinal space, we did not see an increase in apoptotic or necrotic cell death due to the biopolymer, suggesting that the biopolymer did not produce extensive and global retinal toxicity. Our observation that the retina had completely reattached in the injected quadrant of the eye 2-3 weeks post-injection indicates that the biopolymer is non-persistent and is likely cleared by the natural processes of phagocytosis and fluid absorption of the RPE and circulating retinal macrophages. Since 8-10 rows of photoreceptor nuclei were normally present overlying the detachment created by the polymer, we expect complete structural and functional recovery at later time points.

In summary, our study shows that subretinal administration of the adhesive biopolymer has excellent biocompatibility. We found no evidence of retinal toxicity or inflammation from the biopolymer injections using anatomical, histological and functional evaluations. Further studies are needed to confirm the safety and efficacy of this biopolymer for the treatment of retinal detachment in humans.

Acknowledgements

This work is supported by National Eye Institute of the National Institute of Health under award number P30-EY000331-48 to Dr. Steven Nusinowitz. This work is also supported by the Unrestricted Grant from Research to Prevent Blindness, Inc. to the Department of Ophthalmology at UCLA. The authors thank Dr. Gabriel H Travis for providing invaluable laboratory support and encouragement, Dr. Dean Bok for critical review of the manuscript; Samer Habib for assistance with ERG and OCT; Nicholas Bischoff for help in mouse husbandry; Shannan Eddington and Marcia Lloyd for technical contributions.

References

1. Haimann MH, Burton TC, Brown CK. Epidemiology of retinal detachment. Arch Ophthalmol. 1982; 100:289–292. [PubMed: 7065947]
2. Mattioli S, Curti S, De Fazio R, Mt Cooke R, Zanardi F, et al. Occupational lifting tasks and retinal detachment in non-myopics and myopics: extended analysis of a case-control study. Saf Health Work. 2012; 3:52–57. [PubMed: 22953231]

3. Rowe JA, Erie JC, Baratz KH, Hodge DO, Gray DT, et al. Retinal detachment in Olmsted County, Minnesota, 1976 through 1995. Ophthalmology. 1999; 106:154–159. [PubMed: 9917797]
4. Lincoff H, Kreissig I. Changing patterns in the surgery for retinal detachment: 1929 to 2000. Klin Monbl Augenheilkd. 2000; 216:352–359. [PubMed: 10919114]
5. Gonvers M. Temporary silicone oil tamponade in the management of retinal detachment with proliferative vitreoretinopathy. Am J Ophthalmol. 1985; 100:239–245. [PubMed: 4025465]
6. Machemer R, Laqua H. A logical approach to the treatment of massive periretinal proliferation. Ophthalmology. 1978; 85:584–593. [PubMed: 673336]
7. Tiedeman JS. The role of intraocular gases and air in scleral buckling surgery. Semin Ophthalmol. 1995; 10:74–78. [PubMed: 10155700]
8. Yamamoto S, Takeuchi S. Silicone oil and fluorosilicone. Semin Ophthalmol. 2000; 15:15–24. [PubMed: 10749311]
9. Apple DJ, Federman JL, Krolicki TJ, Sims JC, Kent DG, et al. Irreversible silicone oil adhesion to silicone intraocular lenses. A clinicopathologic analysis. Ophthalmology. 1996; 103:1555–1561. [PubMed: 8874426]
10. Casswell AG, Gregor ZJ. Silicone oil removal. II. Operative and postoperative complications. Br J Ophthalmol. 1987; 71:898–902. [PubMed: 3426995]
11. Casswell AG, Gregor ZJ. Silicone oil removal. I. The effect on the complications of silicone oil. Br J Ophthalmol. 1987; 71:893–897. [PubMed: 3426994]
12. Jonas JB, Knorr HL, Rank RM, Budde WM. Retinal redetachment after removal of intraocular silicone oil tamponade. Br J Ophthalmol. 2001; 85:1203–1207. [PubMed: 11567965]
13. Tan HS, Dell'omo R, Mura M. Silicone oil removal after rhegmatogenous retinal detachment: comparing techniques. Eye (Lond). 2012; 26:444–447. [PubMed: 22157918]
14. Coleman DJ, Lucas BC, Fleischman JA, Dennis PH Jr, Chang S, et al. A biologic tissue adhesive for vitreoretinal surgery. Retina. 1988; 8:250–256. [PubMed: 2466319]
15. Hida T, Sheta SM, Proia AD, McCuen BW 2nd. Retinal toxicity of cyanoacrylate tissue adhesive in the rabbit. Retina. 1988; 8:148–153. [PubMed: 3420314]
16. Liggett PE, Cano M, Robin JB, Green RL, Lean JS. Intravitreal biocompatibility of mussel adhesive protein. A preliminary study. Retina. 1990; 10:144–147. [PubMed: 2402556]
17. McCuen BW 2nd, Hida T, Sheta SM, Isbey EK 3rd, Hahn DK, et al. Experimental transvitreal cyanoacrylate retinopexy. Am J Ophthalmol. 1986; 102:199–207. [PubMed: 3740181]
18. Nasaduke I, Peyman GA. The use of autogenous rabbit fibrin sealant to plug retinal holes in experimental detachments. Ann Ophthalmol. 1986; 18:324–327. [PubMed: 2461136]
19. Smiddy WE, Glaser BM, Green WR, Connor TB Jr, Roberts AB, et al. Transforming growth factor beta. A biologic chorioretinal glue. Arch Ophthalmol. 1989; 107:577–580. [PubMed: 2705928]
20. Sueda J, Fukuchi T, Usumoto N, Okuno T, Arai M, et al. Intraocular use of hydrogel tissue adhesive in rabbit eyes. Jpn J Ophthalmol. 2007; 51:89–95. [PubMed: 17401616]
21. Working PK, Newman MS, Johnson J, Cornacoff JB. Safety of poly (ethylene glycol) and poly (ethylene glycol) derivatives. Poly (Ethylene Glycol). 1997; 680:45–57.
22. Knop K, Hoogenboom R, Fischer D, Schubert US. Poly(ethylene glycol) in drug delivery: pros and cons as well as potential alternatives. Angew Chem Int Ed Engl. 2010; 49:6288–6308. [PubMed: 20648499]
23. Ouchi T, Kuroda H, Ohya Y. Design of Antitumor Agent-Terminated Poly(ethylene glycol) Conjugate as Macromolecular Prodrug. Poly(ethylene glycol). 1997; 19:284–296.
24. Askari S, Whirley R. Non-degradable, low swelling, water soluble radiopaque hydrogel polymer. 2006
25. Askari SH, Horng G. Methods for treating diseases of the lung. 2012
26. Askari SH, Horng G. In vivo gelling pharmaceutical pre-formulation. 2012
27. Askari SH, Choi YS. Biocompatible hydrogel treatments for retinal detachment. 2013
28. Kerr M. biomechanical testing of an adhesive polymer intended for the treatment of Retinal Detachment. 2014

29. Nusinowitz S, Ridder WH 3rd, Ramirez J. Temporal response properties of the primary and secondary rod-signaling pathways in normal and Gnat2 mutant mice. Exp Eye Res. 2007; 84:1104–1114. [PubMed: 17408617]
30. Jin M, Li S, Nusinowitz S, Lloyd M, Hu J, et al. The role of interphotoreceptor retinoid-binding protein on the translocation of visual retinoids and function of cone photoreceptors. J Neurosci. 2009; 29:1486–1495. [PubMed: 19193895]
31. Radu RA, Hu J, Yuan Q, Welch DL, Makshanoff J, et al. Complement system dysregulation and inflammation in the retinal pigment epithelium of a mouse model for Stargardt macular degeneration. J Biol Chem. 2011; 286:18593–18601. [PubMed: 21464132]
32. Fisher SK, Lewis GP, Linberg KA, Verardo MR. Cellular remodeling in mammalian retina: results from studies of experimental retinal detachment. Prog Retin Eye Res. 2005; 24:395–431. [PubMed: 15708835]
33. Ning A, Cui J, To E, Ashe KH, Matsubara J. Amyloid-beta deposits lead to retinal degeneration in a mouse model of Alzheimer disease. Invest Ophthalmol Vis Sci. 2008; 49:5136–5143. [PubMed: 18566467]
34. Davies MH, Eubanks JP, Powers MR. Microglia and macrophages are increased in response to ischemia-induced retinopathy in the mouse retina. Mol Vis. 2006; 12:467–477. [PubMed: 16710171]
35. He L, Marneros AG. Macrophages are essential for the early wound healing response and the formation of a fibrovascular scar. Am J Pathol. 2013; 182:2407–2417. [PubMed: 23602833]
36. Hou HY, Wang YS, Xu JF, Wang YC, Liu JP. The dynamic conduct of bone marrow-derived cells in the choroidal neovascularization microenvironment. Curr Eye Res. 2006; 31:1051–1061. [PubMed: 17169844]
37. Xu H, Chen M, Mayer EJ, Forrester JV, Dick AD. Turnover of resident retinal microglia in the normal adult mouse. Glia. 2007; 55:1189–1198. [PubMed: 17600341]
38. Nusinowitz S, Ridder WH, Pang JJ, Chang B, Noorwez SM, et al. Cortical visual function in the rd12 mouse model of Leber Congenital Amarousis (LCA) after gene replacement therapy to restore retinal function. Vision research. 2006; 46:3926–3934. [PubMed: 16814838]
39. Wolfensberger TJ. Jules Gonin. Pioneer of retinal detachment surgery. Indian J Ophthalmol. 2003; 51:303–308. [PubMed: 14750617]
40. Gariano RF, Kim CH. Evaluation and management of suspected retinal detachment. Am Fam Physician. 2004; 69:1691–1698. [PubMed: 15086041]
41. Li X, Beijing Rhegmatogenous Retinal Detachment Study Group. Incidence and epidemiological characteristics of rhegmatogenous retinal detachment in Beijing, China. Ophthalmology. 2003; 110:2413–2417. [PubMed: 14644727]
42. Linsenmeier RA, Padnick-Silver L. Metabolic dependence of photoreceptors on the choroid in the normal and detached retina. Invest Ophthalmol Vis Sci. 2000; 41:3117–3123. [PubMed: 10967072]
43. Mervin K, Valter K, Maslim J, Lewis G, Fisher S, et al. Limiting photoreceptor death and deconstruction during experimental retinal detachment: the value of oxygen supplementation. Am J Ophthalmol. 1999; 128:155–164. [PubMed: 10458170]
44. Kirchhof B, Kirchhof E, Ryan SJ, Sorgente N. Vitreous modulation of migration and proliferation of retinal pigment epithelial cells in vitro. Invest Ophthalmol Vis Sci. 1989; 30:1951–1957. [PubMed: 2777515]
45. Mandelcorn MS, Machemer R, Fineberg E, Hersch SB. Proliferation and metaplasia of intravitreal retinal pigment epithelium cell autotransplants. Am J Ophthalmol. 1975; 80:227–237. [PubMed: 808132]
46. Pastor JC. Proliferative vitreoretinopathy: an overview. Surv Ophthalmol. 1998; 43:3–18. [PubMed: 9716190]
47. Sapieha P, Hamel D, Shao Z, Rivera JC, Zaniolo K, et al. Proliferative retinopathies: angiogenesis that blinds. Int J Biochem Cell Biol. 2010; 42:5–12. [PubMed: 19836461]
48. Chan CK, Lin SG, Nuthi AS, Salib DM. Pneumatic retinopexy for the repair of retinal detachments: a comprehensive review (1986-2007). Surv Ophthalmol. 2008; 53:443–478. [PubMed: 18929759]

49. Hilton GF, Grizzard WS. Pneumatic retinopexy. A two-step outpatient operation without conjunctival incision. Ophthalmology. 1986; 93:626–641. [PubMed: 3523357]
50. Tornambe PE. Pneumatic retinopexy. Surv Ophthalmol. 1988; 32:270–281. [PubMed: 3279561]
51. Lane JI, Watson RE Jr, Witte RJ, McCannel CA. Retinal detachment: imaging of surgical treatments and complications. Radiographics. 2003; 23:983–994. [PubMed: 12853675]
52. Kapany NS, Peppers NA, Zweng HC, Flocks M. Retinal photocoagulation by lasers. Nature. 1963; 199:146–149. [PubMed: 14043179]
53. Paulus YM, Jain A, Gariano RF, Stanzel BV, Marmor M, et al. Healing of retinal photocoagulation lesions. Invest Ophthalmol Vis Sci. 2008; 49:5540–5545. [PubMed: 18757510]
54. Gilbert CE 1, Grierson I, McLeod D. Retinal patching: a new approach to the management of selected retinal breaks. Eye (Lond). 1989; 3:19–26. [PubMed: 2591594]
55. Kerr, MMP. Biomechanical Testing Of An Adhesive Polymer Intended For The Treatment Of Retinal Detachment. University of California; Los Angeles, Ann Arbor: 2014. p. 70
56. Rubin LF. Albino versus pigmented animals for ocular toxicity testing. Lens Eye Toxic Res. 1990; 7:221–230. [PubMed: 2100160]
57. Engelhardt M, Tosha C, Lopes VS, Chen B, Nguyen L, et al. Functional and morphological analysis of the subretinal injection of retinal pigment epithelium cells. Vis Neurosci. 2012; 29:83–93. [PubMed: 22391151]
58. Fisher SK, Erickson PA, Lewis GP, Anderson DH. Intraretinal proliferation induced by retinal detachment. Invest Ophthalmol Vis Sci. 1991; 32:1739–1748. [PubMed: 2032796]
59. Lewis GP, Fisher SK. Up-regulation of glial fibrillary acidic protein in response to retinal injury: its potential role in glial remodeling and a comparison to vimentin expression. International review of cytology. 2003; 230:263–290. [PubMed: 14692684]
60. Paranthan RR, Bargagna-Mohan P, Lau DL, Mohan R. A robust model for simultaneously inducing corneal neovascularization and retinal gliosis in the mouse eye. Mol Vis. 2011; 17:1901–1908. [PubMed: 21850164]
61. Hisatomi T, Sakamoto T, Murata T, Yamanaka I, Oshima Y, et al. Relocalization of apoptosis-inducing factor in photoreceptor apoptosis induced by retinal detachment in vivo. See Am J Pathol. 2001; 158:1271–1278.

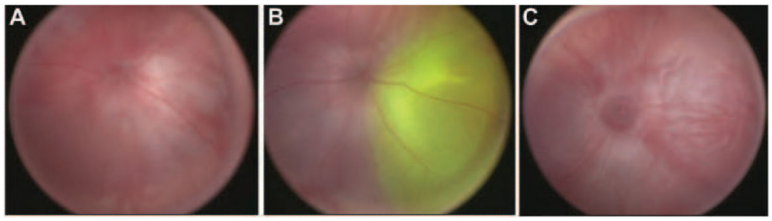

Figure 1.

Color fundus imaging of control and biopolymer injected mice eyes. **(A)** Non-injected wild type mouse fundus. **(B)** Biopolymer, with fluorescein dye injected in the subretinal space at day 0 post-injection. **(C)** Subretinal biopolymer injected eye 1 week post-injection. The fluorescein was absorbed but outline of the bleb can be seen.

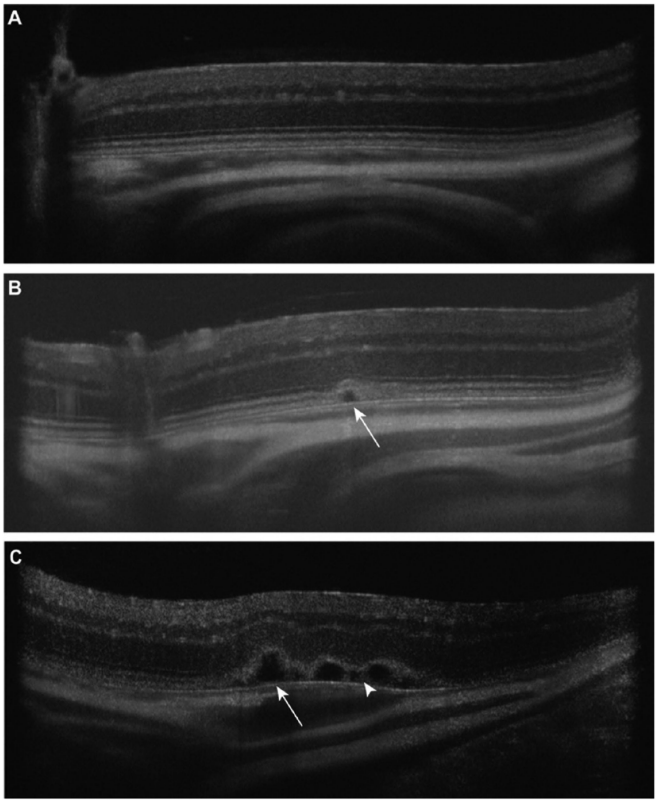

Figure 2.

Spectral domain OCT images of control and injected eyes 1 week post injection. **(A)** Non-injected eye, **(B)** BSS injected and **(C)** subretinal biopolymer injected eyes. Localized disruption of the outer retina is seen at the needle entry point in eyes with subretinal injections of biopolymer as well as BSS (arrows). The BSS bleb is completely resolved, but some biopolymer persists in the subretinal space at 1 week. Photoreceptor outer segment debris created by the injection pressure of the biopolymer is also seen under the retina (arrowhead). Photoreceptor nuclear layer and inner retina appear unaffected.

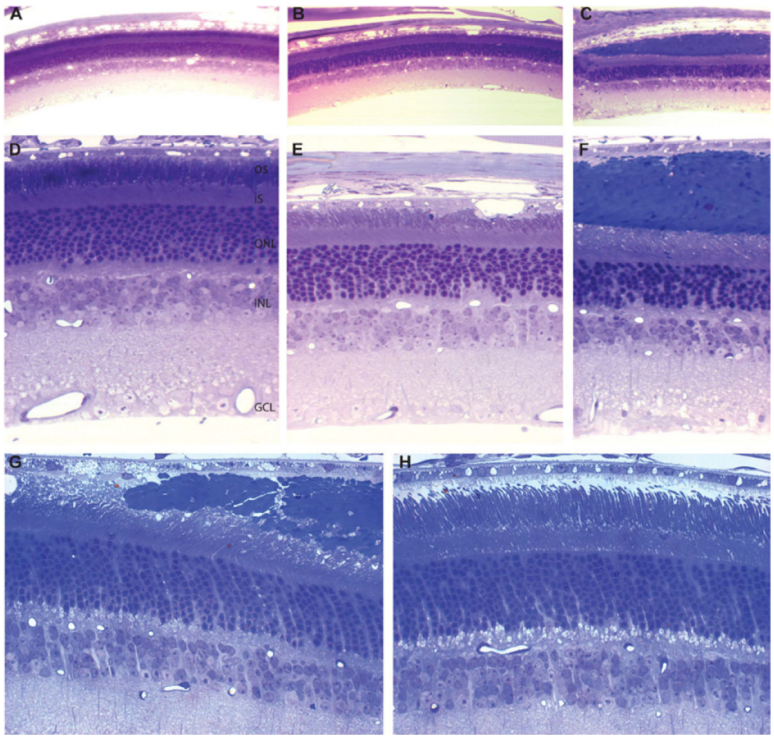

Figure 3.

Plastic-embedded sections of eyes 1 day post-injection stained with Toluidine blue. **(A, D)** Non-injected control eyes. **(B, E)** BSS-injected control eyes. Overall retinal layers appear normal in non-injected and BSS-injected. Some photoreceptor outer segment and RPE abnormalities are observed in BSS-injected eyes. **(C,F,G)** Subretinal biopolymer injected eyes showing retinal detachment. The injected biopolymer is seen in the subretinal space in biopolymer injected eyes with no other retinal abnormalities. Rounded phagocytic cells appear to be infiltrating the biopolymer from the RPE layer. (H) Retina appears completely normal outside the detached area in the subretinal biopolymer-injected eye. OS: Outer Segment Layer; IS: Inner Segment Layer; ONL: Outer Nuclear Layer; INL: Inner Nuclear Layer; GCL: Ganglion Cell Layer.

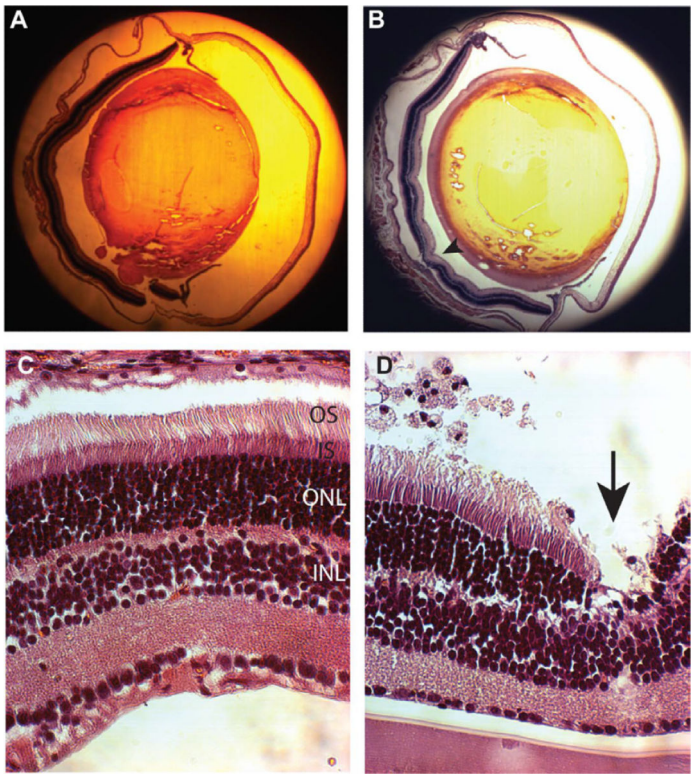

Figure 4.

Formalin fixed paraffin embedded sections of mouse eyes 3 weeks post-injection stained with Haematoxylin-eosin. **(A,C)** BSS-injected control eye. **(B,D)** Subretinal polymer injected eye. Physical damage to the outer retina marks the needle puncture site (arrow) with clumps of rounded displaced RPE/ phagocytic cells in the subretinal space. Retinal layers are normal throughout the entire globe.

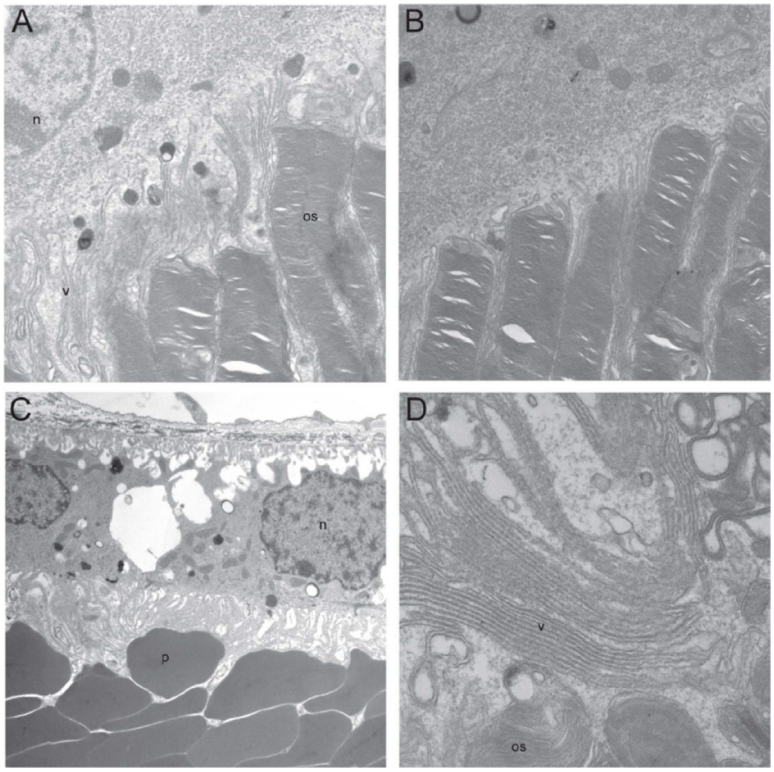

Figure 5.

Transmission electron microscopic images of ultra-thin sections from injected eyes. **(A)** Non-injected control eye section, **(B)** subretinal BSS-injected control eye section, **(C)** subretinal biopolymer-injected 1 day eye section post-injection and **(D)** subretinal biopolymer-injected eye section 3 weeks post-injection. RPE cells from non-injected and BSS-injected controls have long apical microvilli surrounding the photoreceptor outer segment tips. At 1 day post-injection, amorphous biopolymer “blobs” can be seen in the subretinal space adjacent the RPE in biopolymer-injected eye. 3 weeks after injection, the biopolymer has been degraded/absorbed and the RPE microvilli appear to form their normal morphology. os: Photoreceptor Outer Segment; n: Nucleus; v: RPE Microvilli; p: Biopolymer.

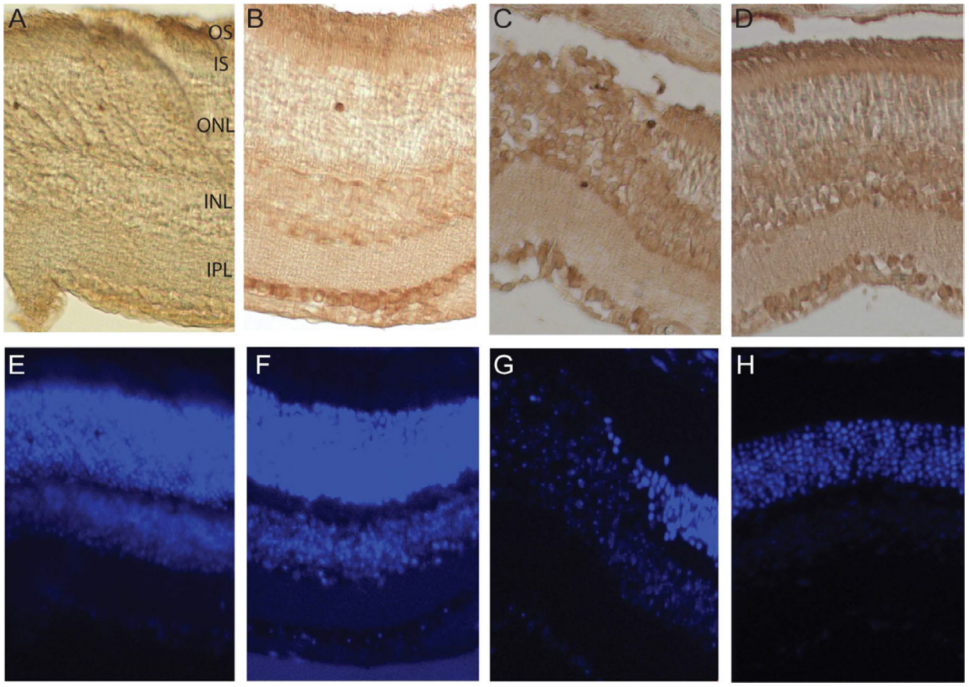

Figure 6.

Terminal deoxynucleotidyl transferase mediated dUTP Nick End Labeling assay (TUNEL) staining to detect apoptotic and necrotic nuclei. **(A)** Non-injected control and **(B)** BSS-injected control eyes have minimal cell death detectable by TUNEL labeling. **(C)** Subretinal polymer injected eyes have apoptotic nuclei mainly in the outer nuclear layer at the needle entry site and no TUNEL positive nuclei were detected outside the injection site **(D)**. Nuclei are stained with DAPI **(E-H)**.

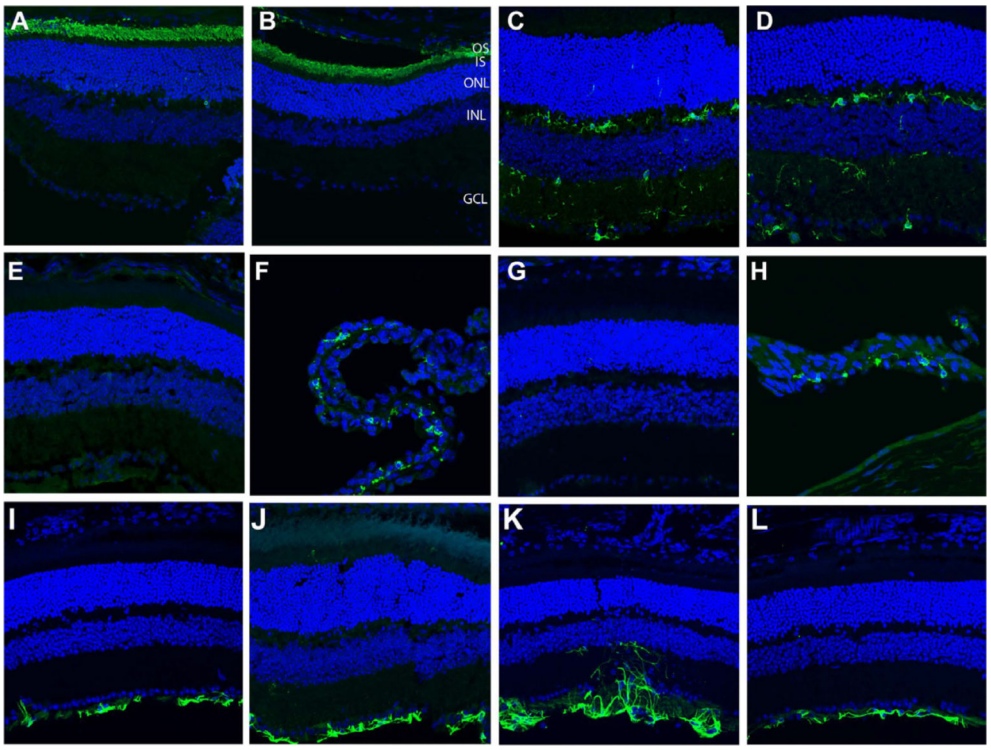

Figure 7.

Immunolocalization of resident retinal proteins and inflammatory markers in subretinal polymer injected eyes and control 1 week post-injection. Rhodopsin immunolabeling shows no difference in localization of rhodopsin in (A) control non-injected and (B) subretinal biopolymer injected eyes. Iba1-positive microglial cells are localized to the ganglion cell layer, inner plexiform layer and outer plexiform layer both (C) control subretinal BSS-injected and (D) subretinal biopolymer-injected eyes. F4/80 immunoreactivity was not observed in either (E) control BSS-injected or (G) subretinal biopolymer eyes. As positive controls, the ciliary body from the same section has F4/80-positive macrophages in both (F) control BSS-injected and (H) subretinal biopolymer-injected eyes. GFAP labeling in (I) non-injected control eye, (J) BSS-injected control eye and (K) subretinal biopolymer-injected eye at the site of needle entry and (L) subretinal biopolymer-injected eye distal to the injection site. Moderate proliferation of GFAP-positive Müller cells is seen at the injection site but not distal to the injection site in subretinal biopolymer eyes.